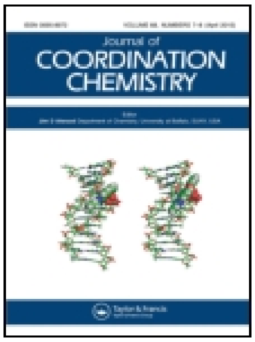

Taylor & Francis
Taylor & Francis Group

Journal of Coordination Chemistry

ISSN: 0095-8972 (Print) 1029-0389 (Online) Journal homepage: http://www.tandfonline.com/loi/gcoo20

Racemic and homochiral coordination polymers based on carboxylates of different lengths

Hong-Qing Hao, Zhi-Cong Chen, Wei-Cong Kuang & Meng-Xia Peng

To cite this article: Hong-Qing Hao, Zhi-Cong Chen, Wei-Cong Kuang & Meng-Xia Peng (2015) Racemic and homochiral coordination polymers based on carboxylates of different lengths, Journal of Coordination Chemistry, 68:15, 2715-2724, DOI: 10.1080/00958972.2015.1058484

To link to this article: http://dx.doi.org/10.1080/00958972.2015.1058484

Journal of Coordination Chemistry, 2015
Vol. 68, No. 15, 2715–2724, http://dx.doi.org/10.1080/00958972.2015.1058484

Racemic and homochiral coordination polymers based on carboxylates of different lengths

HONG-QING HAO*, ZHI-CONG CHEN, WEI-CONG KUANG and MENG-XIA PENG

School of Chemistry and Environment, Jiaying University, Meizhou, PR China

(*Received 17 September 2014; accepted 9 April 2015*)

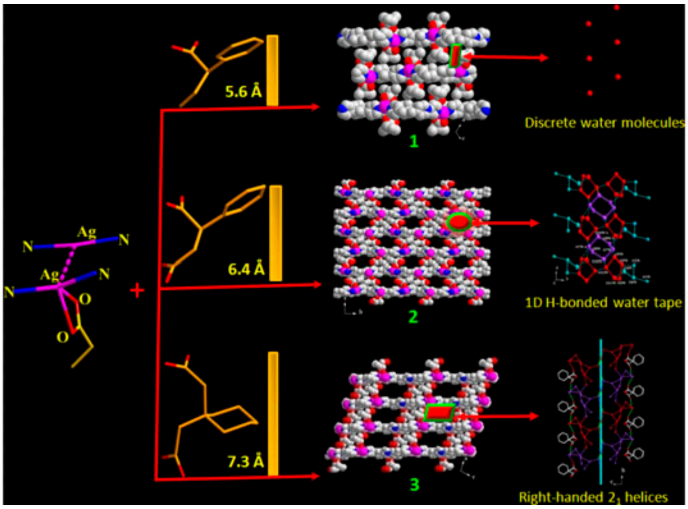

Two racemic and one homochiral 3-D H-bonded supramolecular frameworks constructed from the mutually interdigitated 2-D motifs, showing interesting pore structures and properties, have been synthesized by the solution reactions of Ag(I) with bpp and three carboxylates of different lengths.

Three coordination polymers, $\{[Ag_2(R\text{-PHBU})(S\text{-PHBU})(bpp)_2]\cdot H_2O\}_n$ (**1**, racemic), $\{[Ag_2(R\text{-PHSU})_{0.5}(S\text{-PHSU})_{0.5}(bpp)_2]\cdot 2H_2O\}_n$ (**2**, racemic), and $\{[Ag_2(CHDA)(bpp)_2]\cdot 9H_2O\}_n$ (**3**, homochiral) (HPHBU = 2-phenylbutyric acid, H_2PHSU = 2-phenylsuccinic acid, H_2CHDA = 1,1-cyclohexanediacetic acid, bpp = 1,3-bis(4-pyridyl)propane), have been synthesized by solution reactions of Ag(I) with bpp and *rac*-$PHBU^-$, *rac*-$PHSU^{2-}$, or $CHDA^{2-}$. Single-crystal X-ray diffraction reveals that all three complexes feature "Ag···Ag" subunits extended by bpp ligands in two-dimensional (2-D) $[Ag(bpp)_2]_n^{2n+}$ cation layers, which are embedded by the $PHBU^-$, $PHSU^{2-}$, or $CHDA^{2-}$ ligands of different lengths. Adjacent 2-D layers with pillar-shaped fillers are mutually interdigitated to 3-D H-bonded supramolecular coordination polymers with 1-D pores. As the length of the pillar-shaped fillers increases from 5.6, 6.4 to 7.3 Å, the dimensions of the pores range from 5.0 × 3.7 Å (narrow slit), 8.7 × 5.6 Å (elliptical) to 13.4 × 6.8 Å (quadrangular), and the solvent-accessible void volumes range from 3.6, 31.8 to 36.4% of the crystal volumes. The 1-D pores are filled with guest water molecules. The guest water molecules in **1** are discrete. Centrosymmetric water tapes and

---

*Corresponding author. Emails: hqhao@jyu.edu.cn, hqhao@126.com

chiral right-handed *2₁* helical water tapes are observed in **2** and **3**, respectively. Thermal and photoluminescent properties, as well as lead(II) adsorption, are also discussed.

Keywords: Coordination polymer; H-Bonded; Carboxylate

1. Introduction

Porous coordination polymers have attracted attention owing to intriguing architectures and versatile applications, catalysis, gas storage, magnetism, separation, and exchange of guests in cavities [1, 2]. To date, much effort has been made to develop rigidly porous polymers assembled with coordination bonds [3, 4]. In contrast, limited porous supramolecular coordination polymers constructed by weak interactions have been reported, such as hydrogen bonding, molecule packing, or van der Waals interactions between low-dimensional coordination motifs [5]. Low-dimensional structural motifs could be dynamic and shape-memory materials as they may show structural changes during guest adsorption/desorption or sustain changes caused by external stimuli [6, 7]. Nevertheless, it is still a challenge to construct and control the dynamic nature of porous supramolecular coordination polymers, especially chiral-related materials [8–10].

We have previously reported a series of sandwich-like coordination polymers of Ag_2–RCO_2–bpp (R = phenyl or pyridyl, bpp = 1,3-di(4-pyridyl)propane), which have typical 3-D supramolecular coordination polymers constructed from Ag···Ag interaction directed $\left[Ag_2(N–N)_2\right]_n^{n+}$ coordination ladders or layers linked by carboxylate pillar-shaped fillers [11]. In this work, flexible carboxylates with different lengths and substituent groups ($PHBU^-$, $PHSU^{2-}$, and $CHDA^{2-}$) were introduced (see scheme 1). Two racemic and one homochiral MOF constructed from mutually interdigitated 2-D motifs, showing interesting pore structures and properties, have been synthesized and characterized.

2. Experimental

2.1. *Materials and methods*

Reagents and solvents employed were commercially available and used as received. FT-IR spectra were recorded as KBr pellets from 4000 to 400 cm^{-1} on a Nikolai AVATAR spectrometer. The C, H, and N elemental analyses were carried out with an Elementar Vario–El CHNS analyzer. Thermogravimetric analysis (TGA) was performed at a rate of 10 °C min^{-1} using a SHIMADZU DTG-60 system. The concentration of lead(II) was determined by a INESA-722S spectrophotometer before and after adsorption. The solid-state photoexcitation and emission spectra were performed on a Perkin Elmer LS55 spectrophotometer.

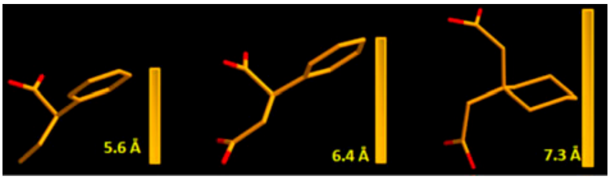

$PHBU^-$ $PHSU^{2-}$ $CHDA^{2-}$

Scheme 1. The length of three pillar-shaped carboxylates.

2.2. *Synthesis*

2.2.1. Synthesis of $\{[Ag_2(R\text{-PHBU})(S\text{-PHBU})(bpp)_2]\cdot H_2O\}_n$ (1). A mixture of $[Ag(NH_3)_2](OH)$ (0.5 mmol), *rac*-HPHBU (0.082 g, 0.5 mmol), bpp (0.05 g, 0.5 mmol), and water (10 mL) was vigorously stirred for 10 min at room temperature. The resulting solution was filtered and allowed to stand in air at room temperature. Block colorless crystals were obtained after three days (yield: 70%). Anal. Calcd for $C_{46}H_{52}N_4O_5Ag_2$: C, 57.75; H, 5.48; N, 5.86. Found: C, 57.84; H, 5.46; N, 5.93. IR (KBr, cm^{-1}): 3430(vs), 3061(w), 2964 (m), 2362(m), 1661(w), 1607(vs), 1572(vs), 1492(w), 1460(m), 1391(s), 1228(m), 1072(w), 1000(w), 807(s), 702(m), 508(m).

2.2.2. Synthesis of $\{[Ag_2(R\text{-PHSU})_{0.5}(S\text{-PHSU})_{0.5}(bpp)_2]\cdot 12H_2O\}_n$ (2). A mixture of $[Ag(NH_3)_2](OH)$ (0.5 mmol), *rac*-H_2PHSU (0.048 g, 0.25 mmol), bpp (0.05 g, 0.5 mmol), and water (15 mL) was vigorously stirred for 10 min at room temperature. The resulting solution was filtered and allowed to stand in air at room temperature. Block colorless crystals were obtained after five days (yield: 80%). Anal. Calcd for $C_{36}H_{60}N_4O_{16}Ag_2$: C, 42.37; H, 5.92; N, 5.49. Found: C, 42.43; H, 5.83; N, 5.56. IR (KBr, cm^{-1}): 3351(m), 3071(w), 2942 (w), 2864(w), 1611(vs), 1552(vs), 1491(w), 1457(m), 1410(vs), 1275(w), 1220(m), 1072 (w), 989(m), 804(s), 698(w), 502(s).

2.2.3. Synthesis of $\{[Ag_2(CHDA)(bpp)_2]\cdot 9H_2O\}_n$ (3). A mixture of $[Ag(NH_3)_2](OH)$ (0.5 mmol), H_2CHDA (0.1001 g, 0.5 mmol), bpp (0.05 g, 0.5 mmol), and water (15 mL) was vigorously stirred for 10 min at room temperature. The resulting solution was filtered and allowed to stand in air at room temperature. Rod-like colorless crystals were obtained after three days (yield: 75%). Anal. Calcd for $C_{36}H_{60}N_4O_{13}Ag_2$: C, 44.46; H, 6.22; N, 5.76. Found: C, 44.35; H, 6.28; N, 5.64. IR (KBr, cm^{-1}): 3383(s), 2921(m), 2847(w), 1647(w), 1589(vs), 1551(vs), 1458(m), 1389(s), 1202(m), 1067(w), 999(m), 791(m), 608(w), 504(m).

2.3. *Crystal structure determination*

Data collections were performed on a Bruker Apex CCD diffractometer with Mo Kα radiation (λ = 0.71073 Å) at 150 K for **1**, **2**, and **3**. The intensities were integrated with SAINT$^+$ and also applied corrections for Lorentz and polarization effects. Absorption corrections were applied by using the multi-scan program SADABS [12]. The structures were solved by direct methods. All non-hydrogen atoms were refined anisotropically by least squares on F^2 using SHELXTL [13]. The organic hydrogens were generated geometrically (C_{aryl}–H 0.93 Å; C_{alkyl}–H 0.97 Å). Crystal data as well as details of data collection and refinements for **1**, **2**, and **3** are summarized in table 1.

3. Results and discussion

3.1. *Synthesis*

Different sources of the reactant components (e.g., utilization of different metal salts and organic precursors instead of target ligands) can greatly influence the crystallization resultant products. Reactions of silver(I) salts and organic ligands with carboxylic groups in aqueous solution often lead to microcrystalline or amorphous insoluble “silver complexes,”

Table 1. Crystal data and structure refinement for **1**, **2**, and **3**.

Compound	1	2	3
Empirical formula	$C_{46}H_{52}N_4O_5Ag_2$	$C_{36}H_{60}N_4O_{16}Ag_2$	$C_{36}H_{60}N_4O_{13}Ag_2$
Formula weight	956.67	1020.62	972.62
Temperature (K)	150 K	150 K	150 K
Wavelength (Å)	0.71073	0.71073	0.71073
Crystal size (mm^3)	0.12 × 0.10 × 0.09	0.20 × 0.14 × 0.14	0.18 × 0.15 × 0.14
Crystal system	Monoclinic	Monoclinic	Monoclinic
Space group	*C2/c*	$P2_1/c$	$P2_1$
Unit cell dimensions (Å, °)			
a	22.685(2)	8.622(2)	11.943(1)
b	9.074(1)	25.685(5)	8.687(1)
c	22.724(2)	20.625(4)	24.158(1)
α	90	90	90
β	112.18(1)	97.571(3)	100.984(2)
γ	90	90	90
Volume ($Å^3$), Z	4331.3(8), 8	4527.8(4), 4	2460.51(9), 2
Calculated density ($Mg\ m^{-3}$)	1.464	1.462	1.288
Absorption coefficient (mm^{-1})	0.953	0.932	0.850
F (0 0 0)	1952	2008	968
Reflections collected	10,620	22,962	20,238
Reflections unique	4239	8859	9568
Completeness (%)	99.9	99.4	99.9
R_{int}	0.0454	0.0242	0.0294
Goodness-of-fit on F^2	1.077	1.044	1.089
$R_1{}^a$ [$I > 2\sigma(I)$]	0.0453	0.0492	0.0597
$wR_2{}^b$ (all data)	0.1294	0.1355	0.1788

[a] $R_1 = \sum ||F_o| - |F_c|| / \sum |F$.

[b] $wR_2 = \left[\sum w(F_o^2 - F_c^2)^2 / \sum w(F_o^2)^2\right]^{\frac{1}{2}}$.

which is presumably due to the formation of polymeric structures via rapid interactions between carboxylic groups and silver ions [14]. There is still a general challenge to grow crystals of desired materials with suitable size for X-ray structural analysis. Controlled release of silver ions may help to slow the formation of silver-organic coordination polymers and yield better single crystals. We used freshly synthesized $[Ag(NH_3)_2](OH)$ to react with multi-carboxylic acid ligands and obtained polymeric coordination compounds [11]. In this study, we used freshly synthesized $[Ag(NH_3)_2](OH)$ to react with *rac*-PHBU$^-$, *rac*-PHSU^{2-}, or CHDA^{2-} and bpp ligands, which is rapid and efficient.

3.2. *Crystal structure of* $\{[Ag_2(R\text{-}PHBU)(S\text{-}PHBU)(bpp)_2]\cdot H_2O\}_n$ *(1)*

X-ray crystallographic analysis reveals that **1** crystallizes in the monoclinic *C2/c* space group. Each asymmetric unit contains one Ag(I), one PHBU$^-$, and one bpp [see figure 1(a)]. Ag(I) has a distorted tetrahedral coordination geometry by coordination with two nitrogens of different bpp ligands and two oxygens of the PHBU$^-$ counterion (Ag1–N = 2.218(1) and 2.218(1) Å; Ag1–O = 2.509(1) and 2.683(2) Å). Adjacent Ag(I) ions are ligated into 1-D $[Ag(bpp)]_n^{n+}$ chains by the bpp ligands of *TT* conformation with a N···N distance of 9.511(2) Å and a dihedral angle of 73.2° between the two pyridyl rings (see figure S1, see online supplemental material at http://dx.doi.org/10.1080/00958972.2015.1058484) [15]. The adjacent $[Ag(bpp)]_n^{n+}$ chains are linked into 2-D $\left[Ag_2(bpp)_2\right]_n^{2n+}$ cation layers by Ag···Ag interactions with the distance of 2.963(1) Å, much shorter than van der Waals radii of two silver ions [16].

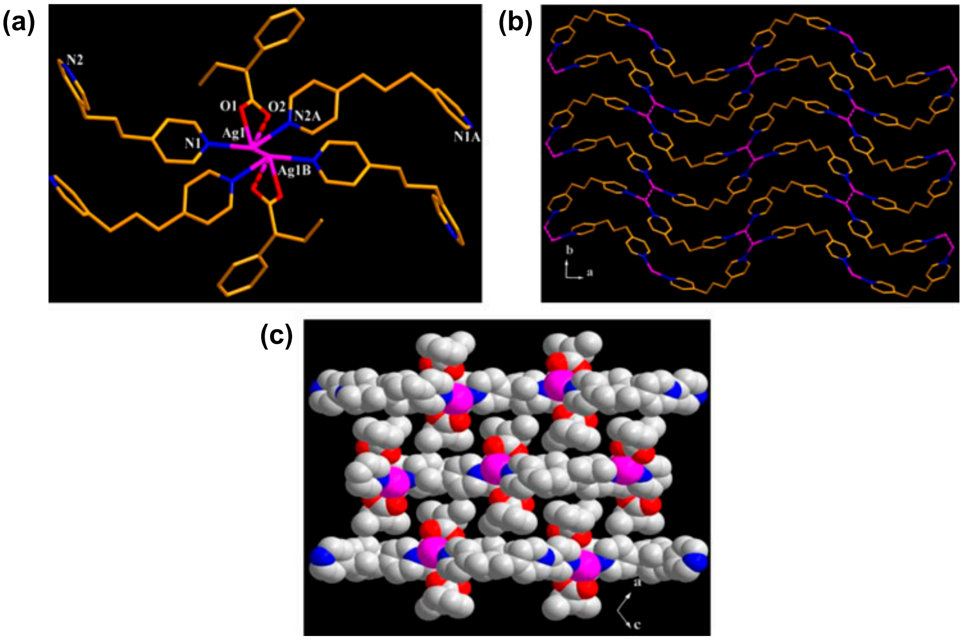

Figure 1. (a) Coordination environment of Ag(I) (symmetry codes: (A) $x-1/2$, $1/2-y$, $z-1/2$; (B) $-x$, $-y$, $-z$), (b) the $[Ag_2(bpp)_2]_n^{2n+}$ layer with Ag···Ag interactions, and (c) space-filling model of the 3-D supramolecular coordination polymer with 1-D narrow slit pores along the *b*-axis in **1**.

The resulting 2-D $[Ag_2(bpp)_2]_n^{2n+}$ cation layer extends on the crystallographic *ab* plane [see figure 1(b)]. The $[Ag_2(bpp)_2]_n^{2n+}$ layers are vertically embedded by $PHBU^-$ pillar-shaped fillers. The successive $[Ag(bpp)]_n^{n+}$ chains are inversion-related and thus contain the same amount of *R*-$PHBU^-$ and *S*-$PHBU^-$. Upon stacking, the adjacent layers with *rac*-$PHBU^-$ pillar-shaped fillers are mutually interdigitated by hydrogen bonding to give a racemic 3-D H-bonded supramolecular framework with 1-D narrow slit pores along the *b*-axis with dimensions of 5.0 × 3.7 Å [see figure 1(c)]. The narrow slit pores are filled with discrete guest water molecules. The estimated solvent-accessible void volume is 153.9 $Å^3$ per unit cell, which is 3.6% of the unit cell volume, calculated by PLATON [17].

3.3. *Crystal structure of* $\{[Ag_2(\text{R-}PHSU)_{0.5}(\text{S-}PHSU)_{0.5}(bpp)_2]\cdot 12H_2O\}_n$ *(2)*

Compound **2** crystallizes in the monoclinic $P2_1/c$ space group. Each asymmetric unit contains one dimeric $[Ag_2(bpp)_2]^{2+}$ cation, one coordinated $PHSU^{2-}$, and twelve guest water molecules. Both Ag (I) ions (Ag1 and Ag2) have *T*-shaped coordination geometry [see figure 2(a)], linked by two bpp ligands of *TT* conformation with a N···N distance of 9.683 Å and a dihedral angle of 64.9° between the two pyridyl rings (see figure S1) [15] and form an infinite $[Ag(bpp)]_n^{n+}$ chain along the *b*-axis [Ag1–N = 2.191(2) and 2.185(2) Å; Ag2–N = 2.110(2) and 2.105(2) Å]. The adjacent $[Ag(bpp)]_n^{n+}$ chains are aligned parallel and bridged into a 2-D coordination layer by carboxylate groups from one side of $PHSU^{2-}$ [Ag1–O1 = 2.494(1) Å; Ag2–O2 = 2.770(1) Å)]. The Ag···Ag separation is 2.963(1) Å. The *R*-$PHSU^{2-}$ and *S*-$PHSU^{2-}$ ligands stand alternatively on both sides of the coordination

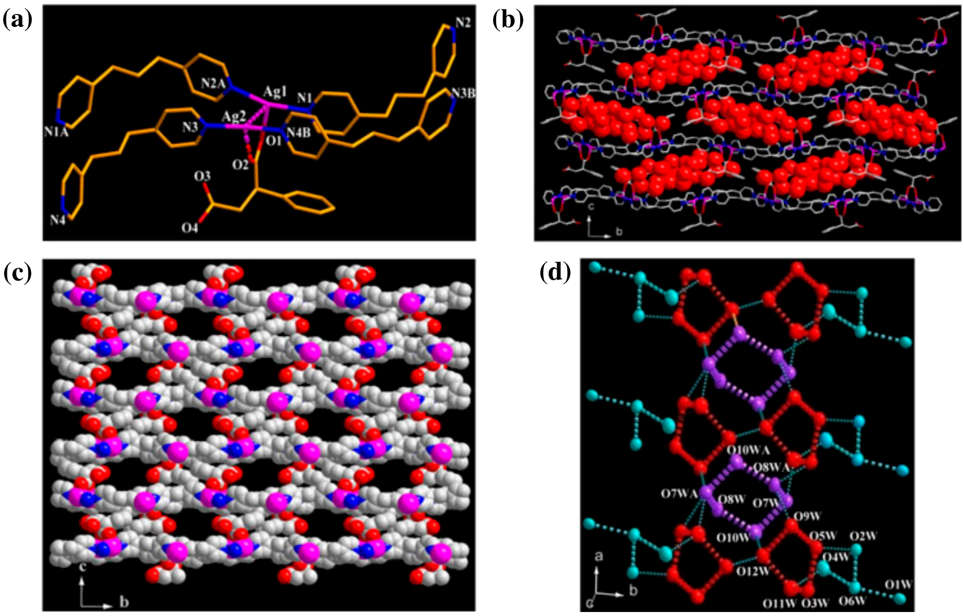

Figure 2. (a) Coordination environment of Ag(I) (symmetry codes: (A) $1-x$, $1/2+y$, $1/2-z$; (B) $-x$, $y-1/2$, $1/2-z$), (b) 3-D supramolecular coordination polymer encapsulating 1-D hydrogen-bonded water tapes, (c) space-filling model of the 3-D supramolecular coordination polymer with 1-D elliptical pores along the *a*-axis, and (d) the 1-D water tape consisting of *T*-shaped $(H_2O)_4$ tetramer, cyclic $(H_2O)_5$ pentamer, and chair-shaped $(H_2O)_6$ hexamer clusters in **2**.

layer along the silver-pyridine chains. The adjacent 2-D motifs with *rac*-PHBU$^-$ pillar-shaped fillers are mutually interdigitated to give a racemic 3-D H-bonded supramolecular framework with 1-D elliptical pores along the *a*-axis with dimensions of 8.7 × 5.6 Å [see figure 2(b) and (c)]. The estimated solvent-accessible void volume is 1441.4 Å^3 per unit cell, which is 31.8% of the unit cell volume. The inside walls of the elliptical-shaped pore are composed of Ag(I) ions, bpp, and *R*-PHSU^{2-} and *S*-PHSU^{2-}. The combination of the pore dimensions and presence of uncoordinated carboxyl groups of *R*-PHSU^{2-} and *S*-PHSU^{2-} lead to a *T*-shaped $(H_2O)_4$ tetramer, cyclic $(H_2O)_5$ pentamer, and chair-shaped $(H_2O)_6$ hexamer in the elliptical pores. Interestingly, the $(H_2O)_4$, $(H_2O)_5$, and $(H_2O)_6$ clusters are further connected into 1-D centrosymmetric water tapes by hydrogen bonding [see figure 2(d)].

3.4. *Crystal structure of* $\{[Ag_2(CHDA)(bpp)_2]\cdot 9H_2O\}_n$ *(3)*

Compound **3** crystallizes in the monoclinic $P2_1$ space group and features a 3-D interdigitated homochiral H-bonded supramolecular framework of achiral ligands. Each asymmetric unit contains two crystallographically distinctive Ag(I) ions (Ag1 and Ag2), one bpp ligand of *TT* conformation with a N···N distance of 9.717 Å, and a dihedral angle of 70.4° between the two pyridyl rings, one bpp ligand of *TG* conformation with a N···N distance of 8.823 Å and a dihedral angle of 78.9° between the two pyridyl rings (see figure S1), one coordinated CHDA^{2-}, and guest water molecules. Ag1 displays a distorted tetrahedral coordination geometry by coordination with one nitrogen of *TT*-bpp, one nitrogen of

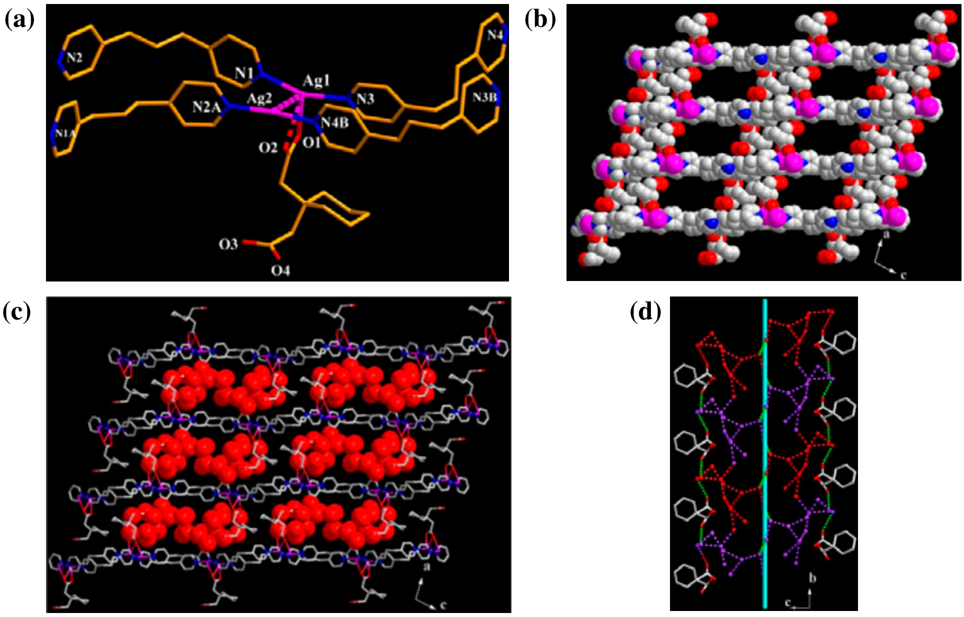

Figure 3. (a) Coordination environment of Ag(I) (symmetry codes: (A) $-x$, $1/2+y$, $-1-z$; (B) $1-x$, $1/2+y$, $-z$), (b) space-filling model of the 3-D supramolecular coordination polymer with 1-D quadrangular pores along the *b*-axis, (c) the 3-D supramolecular coordination polymer encapsulating the hydrogen-bonded 2_1 helical water tape, and (d) hydrogen-bonded 2_1 helical tape along the *b*-axis in **3**.

TG-bpp, and two oxygens of CHDA^{2-} [Ag1–N = 2.147(7) and 2.188(6) Å; Ag1–O = 2.525 (5) and 2.661(2) Å]. Ag2 adopts an unsaturated linear coordination with one nitrogen of *TT*-bpp and one nitrogen of *TG*-bpp [Ag2–N = 2.134(7) and 2.142(7) Å] [see figure 3(a)]. Both Ag1 and Ag2 form an infinite $[\mathrm{Ag(bpp)}]_n^{n+}$ chain along the *b*-axis. The adjacent and parallel $[\mathrm{Ag(bpp)}]_n^{n+}$ chains are bridged into a 2-D coordination layer by Ag···Ag interactions [Ag1···Ag2 = 3.047(1) Å]. The CHDA^{2-} ligands only coordinate to Ag1-pyridine chains, standing on both sides of the coordination layer; the adjacent motifs with CHDA^{2-} pillar-shaped fillers are interdigitated by hydrogen bonding to give a 3-D H-bonded supramolecular framework with 1-D quadrangular pores along the *b*-axis with dimensions of 13.4 × 6.8 Å [see figure 3(b) and (c)]. The estimated solvent-accessible void volume is 894.5 Å^3 per unit cell, which is 36.4% of the unit cell volume.

The coordinated CHDA^{2-} on adjacent Ag1-pyridine chains extends helically in the same direction and forms a 1-D hydrogen-bonded 2_1 helical tape with guest water molecules along the *b*-axis between the layers. Each helical step contains one coordinated CHDA^{2-} linked by 13 water molecules [see figure 3(d)]. All the hydrogen-bonded 2_1 helical tapes are of right-hand (*P*). The 2_1 helical tape of only right-hand direction indicates chiral characteristics of the whole framework. The adjacent 2-D $\left[\mathrm{Ag_2(bpp)_2}\right]_n^{2n+}$ layers are interconnected by the right-handed hydrogen-bonded helical tapes into a homochiral coordination polymer in space group $P2_1$ (Flack parameter: −0.04). We can only detect the configuration with flack parameter of negative in the products. The result is consistent with a case of chiral symmetry breaking [18] *versus* a conglomerate [11(b)].

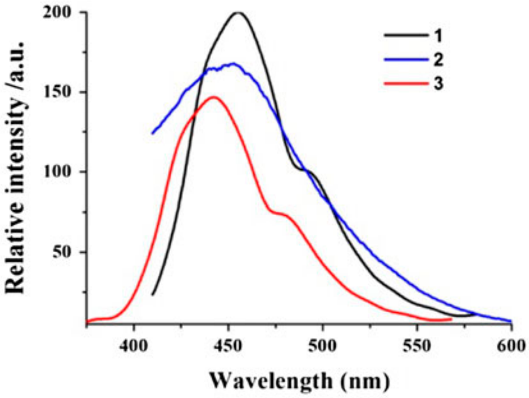

Figure 4. Solid-state emission spectra of **1–3** at ambient temperature.

3.5. *Thermal, photoluminescent, and adsorption properties*

To estimate the stability of the coordination polymers, TGA experiments were performed (see figure S2). In the TG curve of **1**, the first weight loss of 2.0% at 40–75 °C corresponds to the removal of one guest water per formula unit (Calcd 1.9%). For **2**, the first weight loss of 20.7% below 130 °C is attributed to loss of the twelve guest water molecules (Calcd 21.2%). For **3**, the weight loss of 17.0% below 115 °C is attributed to loss of the nine guest water molecules (Calcd 16.7%).

The photoluminescence properties of **1–3** in the solid state were investigated at room temperature (see figure 4). **1** exhibits a broad emission at 455 nm upon excitation at 350 nm. **2** exhibits photoluminescent emission with a maximum at 452 nm upon excitation at 233 nm. **3** presents an emission at 445 nm (λ_{ex} = 378 nm). The fluorescent emissions of **1–3** may be assigned to intraligand transition of coordinated bpp ligands; similar emissions have been observed [19].

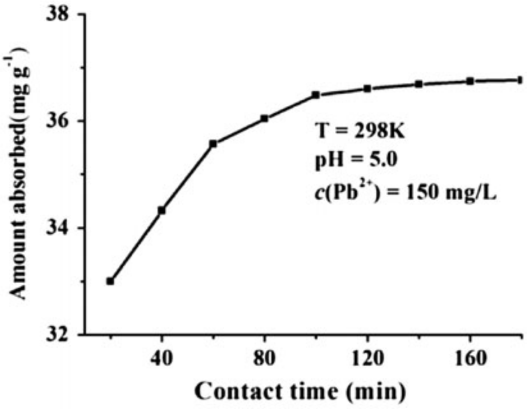

Figure 5. Adsorption curve of lead(II) in aqueous solution by **3**.

We attempted adsorption experiments of lead(II) in aqueous solution by **3**. The effects of contact time, initial concentration of lead(II), and pH were investigated. Results showed that it reached the maximum capacity of 36.5 mg g^{-1} (adsorption efficiency: 91.2%) at 298 K and the pH 5.0, with an initial lead(II) concentration of 150 mg L^{-1} (see figure 5).

4. Conclusion

We have synthesized two racemic and one homochiral H-bonded supramolecular framework based on "Ag···Ag" subunits and pillar-shaped carboxylates of different lengths, which are constructed from mutually interdigitated 2-D motifs. The pore metrics of three coordination polymers can be continuously varied with the length and shape of the carboxylates. Compared with other coordination complexes with carboxylate ligands [20], the arc length and shape of the flexible carboxylates proves important to the 3-D supramolecular frameworks constructed from the mutually interdigitated 2-D motifs. Interestingly, three host coordination polymers encapsulate discrete water molecules, centrosymmetric water tapes and chiral right-handed 2_1 helical water tapes, respectively. Thermal and photoluminescent properties, as well as lead(II) adsorption, have also been discussed. The results may provide opportunities to further study dynamic coordination polymers with flexible linkers and pillars, as well as chirality transfer between coordination polymers and guest molecules.

Supplementary material

Supplementary material available: TGA and IR for **1**, **2**, and **3**. Crystallographic information of **1**, **2**, and **3** has been deposited with the Cambridge Crystallographic Data Center (CCDC) numbers 956328, 956329, and 956946. These data can be obtained free of charge from the Cambridge Crystallographic Data Center via www.ccdc.cam.ac.uk/data_request/cif.

Disclosure statement

No potential conflict of interest was reported by the authors.

Funding

This work was supported by the NSFC [grant number 21101077], the Characteristic Innovation Foundation of Guangdong, China [grant number 2014KTSCX174], and Foundation for Distinguished Young Teachers in Higher Education of Guangdong, China [grant number Yq2013151].

References

[1] (a) Y. Sakata, S. Furukawa, M. Kondo, K. Hirai, N. Horike, Y. Takashima, H. Sakata, N. Kitagawa. *Science*, **339**, 193 (2013); (b) J.P. Zhang, Y.B. Zhang, J.B. Lin, X.M. Chen. *Chem. Rev.*, **112**, 1001 (2012); (c) C. Wang, T. Zhang, W.B. Lin. *Chem. Rev.*, **112**, 1084 (2012); (d) X.L. Wang, C. Qin, E.B. Wang, L. Xu, Z.M. Su, C.W. Hu. *Angew. Chem. Int. Ed.*, **43**, 5036 (2004).

[2] (a) J. Lu, J.X. Lin, M.N. Cao, R. Cao. *Coord. Chem. Rev.*, **257**, 1334 (2013); (b) H.B. Xu, B.W. Wang, F. Pan, Z.M. Wang, S. Gao. *Angew. Chem. Int. Ed.*, **46**, 7388 (2007); (c) S. Supriya, S.K. Das. *New J. Chem.*, **27**, 1568 (2003).

[3] (a) Y. Takashima, V.M. Martinez, S. Furukawa, M. Kondo, S. Shimomura, H. Uehara, M. Nakahama, K. Sugimoto, S. Kitagawa. *Nat. Commun.*, **2**, 168 (2011); (b) H.X. Deng, S. Grunder, K.E. Cordova, C. Valente, H. Furukawa, M. Hmadeh, F. Gándara, A.C. Whalley, Z. Liu, S. Asahina, H. Kazumori, M. O'Keeffe, O. Terasaki, J.F. Stoddart, O.M. Yaghi. *Science*, **336**, 1018 (2012); (c) D.Q. Yuan, W.G. Lu, D. Zhao, H.-C. Zhou. *Adv. Mater.*, **23**, 3723 (2011).

[4] (a) G. Seeber, G.J.T. Cooper, G.N. Newton, M.H. Rosnes, D.L. Long, B.M. Kariuki, P. Kogerler, L. Cronin. *Chem. Sci.*, **1**, 62 (2010); (b) M.H. Zeng, Q.X. Wang, Y.X. Tan, S. Hu, H.X. Zhao, L.S. Long, M. Kurmoo. *J. Am. Chem. Soc.*, **132**, 2561 (2010).

[5] (a) S. Kitagawa, K.J. Uemura. *Chem. Soc. Rev.*, **34**, 109 (2005); (b) D. Bradshaw, J.B. Claridge, E.J. Cussen, T.J. Prior, M.J. Rosseinsky. *Acc. Chem. Res.*, **38**, 273 (2005); (c) X.M. Liu, R.B. Lin, J.P. Zhang, X.M. Chen. *Inorg. Chem.*, **51**, 5686 (2012).

[6] (a) H.K. Arslan, O. Shekhah, D.C.F. Wieland, M. Paulus, C. Sternemann, M.A. Schroer, S. Tiemeyer, M. Tolan, R.A. Fischer, C. Woll. *J. Am. Chem. Soc.*, **133**, 8158 (2011); (b) C.C. Wang, C.C. Yang, C.T. Yeh, K.Y. Cheng, P.C. Chang, M.L. Ho, G.H. Lee, W.J. Shih, H.S. Sheu. *Inorg. Chem.*, **50**, 597 (2011); (c) C.P. Li, J. Chen, P.W. Liu, M. Du. *CrystEngComm*, **15**, 9713 (2013).

[7] (a) L.S. Long. *CrystEngComm*, **12**, 1354 (2010); (b) Z. Jin, H.Y. Zhao, X.J. Zhao, Q.R. Fang, J.R. Long, G.S. Zhu. *Chem. Commun.*, **46**, 8612 (2010).

[8] (a) K. Mo, Y.H. Yang, Y. Cui. *J. Am. Chem. Soc.*, **136**, 1746 (2014); (b) Z.J. Li, J. Yao, Q. Tao, L. Jiang, T.B. Lu. *Inorg. Chem.*, **52**, 11694 (2013); (c) X. Jing, C. He, D. Dong, L. Yang, C.Y. Duan. *Angew. Chem. Int. Ed.*, **51**, 10127 (2012).

[9] (a) V. Colombo, S. Galli, H.J. Choi, G.D. Han, A. Maspero, G. Palmisano, N. Masciocchi, J.R. Long. *Chem. Sci.*, **2**, 1311 (2011); (b) B. Liu, H.B. Zheng, Z.M. Wang, S. Gao. *CrystEngComm*, **13**, 5285 (2011).

[10] (a) J. Liu, Y.X. Tan, F. Wang, Y. Kang, J. Zhang. *CrystEngComm*, **14**, 789 (2012); (b) Y.J. Lin, F. Zou, S.G. Wan, J. Ouyang, L.R. Lin, H. Zhang. *Dalton Trans.*, **41**, 6696 (2012).

[11] (a) H.Q. Hao, W.T. Liu, W. Tan, Z. Lin, M.L. Tong. *Cryst. Growth Des.*, **9**, 457 (2009); (b) H.Q. Hao, W.T. Liu, W. Tan, Z. Lin, M.L. Tong. *CrystEngComm*, **11**, 967 (2009); (c) H.Q. Hao, M. Peng, L. Li. *Inorg. Chem. Commun.*, **20**, 263 (2012).

[12] G.M. Sheldrick. *SADABS 2.05*, University Göttingen, Göttingen (1996).

[13] *SHELXTL 6.10*, Bruker Analytical Instrumentation, Madison, WI (2000).

[14] (a) A. Michaelides, V. Kiritsis, S. Skoulika, A. Aubry. *Angew. Chem. Int. Ed.*, **32**, 1495 (1993); (b) X. Zhang, G.C. Guo, F.K. Zheng, G.W. Zhou, J.G. Mao, Z.C. Dong, J.S. Huang, T.C.W. Mak. *Dalton Trans.*, 1344, (2002).

[15] (a) L. Carlucci, G. Ciani, D.M. Proserpio, S. Rizzato. *CrystEngComm*, **4**, 121 (2002); (b) G.P. Yang, L. Hou, X.J. Luan, B. Wu, Y.Y. Wang. *Chem. Soc. Rev.*, **41**, 6992 (2012).

[16] (a) A.J. Bondi. *J. Phys. Chem.*, **68**, 441 (1964); (b) P. Pyykkö. *Chem. Rev.*, **97**, 597 (1997).

[17] A.L. Spek. *J. Appl. Crystallogr.*, **36**, 7 (2003).

[18] (a) H.Q. Hao, C. Wang, Z. Chen. *Inorg. Chem. Commun.*, **49**, 151 (2014); (b) S. Wu, Y. Wu, Q. Kang, H. Zhang, L.S. Long, Z.P. Zheng, R.B. Huang, L.S. Zheng. *Angew. Chem. Int. Ed.*, **46**, 8475 (2007).

[19] G. Wu, X.F. Wang, T.A. Okamura, W.Y. Sun, N. Ueyama. *Inorg. Chem.*, **45**, 8523 (2006).

[20] (a) S. Xiao, Y. Zhao, C. He, G.H. Cui. *J. Coord. Chem.*, **66**, 89 (2013); (b) L. Sun, J.F. Song, R.S. Zhou, J. Zhang, K.L. Cui, X.Y. Xu. *J. Coord. Chem.*, **67**, 822 (2014); (c) N. Wang, X. Yu, X. Zhang, W. Gao, R. Xin, H. Zhang, Y. Yang, X. Qiu. *J. Coord. Chem.*, **67**, 837 (2014); (d) F.J. Yin, H. Zhao, X.Y. Xu, M.W. Guo. *J. Coord. Chem.*, **66**, 3199 (2013).